

Estimating Atmospheric Dust Pollutants Content Deposited on Snow Surfaces From In Situ Spectral Reflectance Measurements and Satellite Data

Donghang Shao¹, Hongyi Li¹, Alexander Kokhanovsky², Wenzheng Ji¹, Xinyue Zhong¹, Haojie Li¹, Hongxing Li¹, and Xiaohua Hao¹

Abstract—Dust deposited on the surface of snow and glaciers can significantly reduce the snow and ice albedo and accelerate melting. Manual observations of the dust mass concentration (DMC) on snow and glacier surfaces are routinely performed at many locations worldwide. However, snow and ice surface DMC monitoring methods based on remote sensing data still face challenges. This study presents a new retrieval scheme for estimating dust load on snow-covered surfaces from a moderate-resolution imaging spectroradiometer and visible infrared imaging radiometer suite in Northeast and Northwest China that utilizes a classical snow radiative transfer model. Our results indicate that the coefficient of variation of DMC retrieved from the in situ measurements of snow spectral reflectance is 4%, which is within a +4% difference compared with DMC observed in snow and ice samples. Estimating atmospheric dust pollutants content deposited on snow surfaces based on satellite remote sensing observations is feasible. In Northwest China, the root-mean-square error (RMSE) of the DMC values retrieved from VNP09GA data is 9.78 ppm, while that of the DMC values retrieved from MOD09GA data is 13.74 ppm. In Northeast China, the RMSE of the DMC values retrieved from VNP09GA data is 73.98 ppm, while that of the DMC values retrieved from MOD09GA data is 184.32 ppm. The research results can realize continuous monitoring of the atmospheric dust pollutants deposited on snow surfaces, which is of great practical significance to understanding and studying the pollution process of atmospheric dust on snow.

Manuscript received 8 January 2024; revised 26 February 2024; accepted 19 March 2024. Date of publication 25 March 2024; date of current version 12 April 2024. This work was supported in part by the National Natural Science Foundation of China under Grant 42201153 and Grant 42271147, in part by Second Tibetan Plateau Scientific Expedition and Research (STEP) Program under Grant 2019QZKK020109, in part by EnMAP Science Program under the Space Agency at the DLR with resources from the German Federal Ministry of Economic Affairs and Climate Action under Grant 50EE1923, and in part by Gansu Provincial Youth Science and Technology Fund Projects under Grant 23JRRA595. (Corresponding author: Xiaohua Hao.)

Donghang Shao, Hongyi Li, Wenzheng Ji, Xinyue Zhong, and Xiaohua Hao are with the Key Laboratory of Remote Sensing of Gansu Province, Heihe Remote Sensing Experimental Research Station, Northwest Institute of Eco-Environment and Resources, Chinese Academy of Sciences, Lanzhou 730000, China (e-mail: shaodonghang@lzb.ac.cn; lihongyi@lzb.ac.cn; jiwenzheng@neer.ac.cn; xyzhong@lzb.ac.cn; haoxh@lzb.ac.cn).

Alexander Kokhanovsky is with the German Research Centre for Geosciences, 14473 Potsdam, Germany (e-mail: alexander.kokhanovsky@gfz-potsdam.de).

Haojie Li is with the College of Geography and Environmental Science, Northwest Normal University, Lanzhou 730070, China (e-mail: lihaojie@lzb.ac.cn).

Hongxing Li is with the National Cryosphere Desert Data Center, Northwest Institute of Eco-Environment and Resources, Chinese Academy of Sciences, Lanzhou 730000, China (e-mail: lihongxing@lzb.ac.cn).

Digital Object Identifier 10.1109/JSTARS.2024.3381009

Index Terms—Atmospheric dust pollutants, dust mass concentration (DMC), light-absorbing impurity, remote sensing, snow.

I. INTRODUCTION

IN THE 20th century, climate change-induced drought and human land-use development led to an almost doubling of the atmospheric dust content [1]. In downwind regions of large-scale drought or semiarid environments, a significant amount of light-absorbing dust is deposited on snow and glacier surfaces due to atmospheric circulation [2]. This deposition notably reduces the albedo of snow and ice surfaces, subsequently causing changes in radiative forcing. The effect of dust on the snow and glacier albedo and melting is becoming increasingly pronounced within the context of climate change [3]. The role of dust is evident in the spatial heterogeneity of snowmelt and snowline trends in high mountain Asia, and the contribution of dust to the snowmelt process increases under snowline rise and climate warming [4], [5], [6]. In snow-covered and glacial areas in Asia, dust is deposited more frequently due to climate change and human activities [7]. Widespread dust deposition onto snow/ice surfaces causes them to darken (see Fig. 1). The ability of snow/ice surfaces to reflect solar radiation flux is reduced, and the amount of solar radiation absorbed increases, which raises the land surface temperature and causes further climate warming [8]. The resulting accelerated melting in snow-covered and glacial areas due to dust deposition threatens the stable supply of ice and snow water resources at the regional scale, thus amplifying regional water shortages. Therefore, obtaining high-precision spatial and temporal continuous dust content information on snow and ice surfaces not only contributes to the sustainable use of ice and snow water resources but also contributes to snow status initialization in regional climate change simulations.

Many studies have shown that numerous dust deposits exist on snow and ice surfaces in high mountain Asia [9], [10], [11]. In Northwest China, the average dust mass concentration (DMC) on snow and ice surfaces is 17.3 ppm [12]. In Northeast China, the average DMC on snow and ice surfaces reaches as high as 1419.6 ppm due to human activities [13]. On the Tibetan Plateau, the DMC in snow and glaciers reaches as high as 846 ppm [14]. There is abundant evidence that dust is the essential source of light-absorbing particles in snow and ice across the Tibetan Plateau and Asia, and its radiative forcing and climatic effects

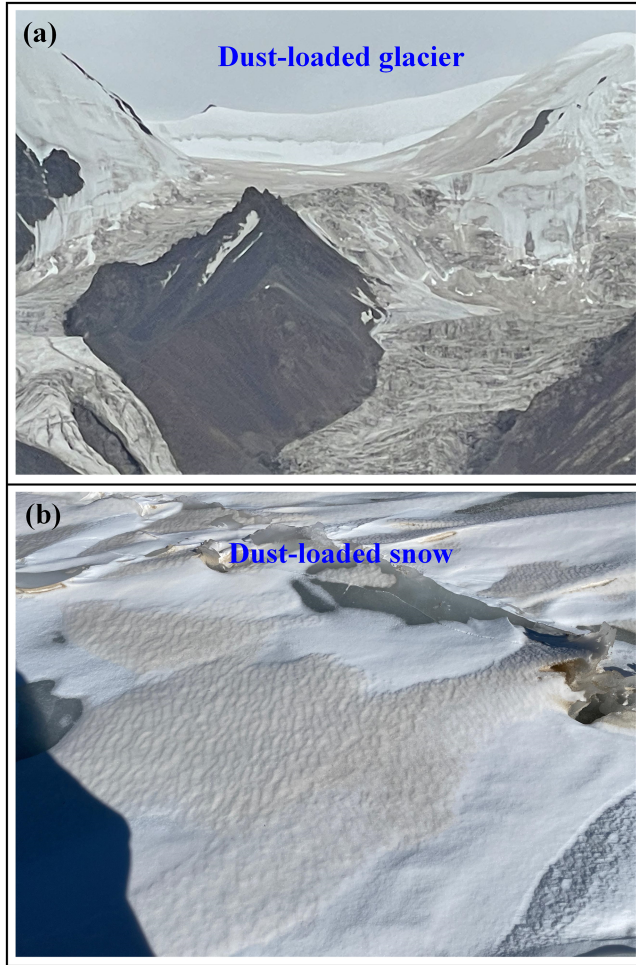


Fig. 1. Dust-covered snow and glaciers in Northwest China. (a) shows the dust-loaded glacier. (b) shows the dust-loaded snow.

on the snow and ice albedo are considerable [14], [15], [16], [17].

At present, three methods are commonly used to obtain the DMC on snow and ice surfaces:

- 1) field sampling and laboratory analysis;
- 2) estimations via the regional weather research and forecasting model coupled with chemistry (WRF-Chem) air quality model;
- 3) satellite remote sensing retrieval.

Field sampling is the most commonly used method to obtain the DMC in snow and ice layers. Many observation experiments have been conducted in various regions, such as the Arctic [9], Antarctic [18], [19], North America [20], southern Europe [21], and the Himalayan-Tibetan Plateau [10], [14], [22]. Despite the high accuracy of field sampling, DMC data are still unavailable for most complex terrains. Most field survey data are derived from single-point observation experiments of snow pits in specific glaciers, which provides data with a very poor spatial resolution. Furthermore, the uncertainty in sampling guidelines and the inherent limitations of analysis equipment can lead to significant variations in the results obtained by researchers within the same region [16]. In addition, field sampling does

not allow for a long time series of observations, limiting its application in hydrological and climate studies. Another way to obtain the DMC on snow and ice surfaces is to employ the WRF-Chem model, which couples meteorological conditions and chemical processes [23]. The WRF-Chem model enables the simulation of dust transport processes, emission fluxes, and DMC levels [24], [25], [26]. However, WRF-Chem model simulations focus on dust aerosols, and it is difficult to accurately obtain information regarding the concentration of dust deposited onto snow and ice surfaces. Satellite remote sensing retrieval can be adopted to effectively obtain spatiotemporally continuous DMC values for snow and ice surfaces. In previous studies, the retrieval of light-absorbing particles on snow and ice surfaces has primarily focused on black carbon concentrations [27], [28], [29], [30], while few studies have focused on DMC retrieval for snow and ice surfaces. In recent years, Kokhanovsky et al. [31] proposed a theoretical physical model based on asymptotic radiative transfer (ART) theory that can be used to retrieve the DMC, snow grain size, and dust mass absorption coefficient for snow and ice surfaces. This model bridges the gap in algorithms for retrieving the dust load on snow and ice surfaces. However, this model has only been applied to in situ snow spectral reflectance measurements at three wavelengths in the visible and near-infrared bands for theoretical retrieval of the dust load on snow and ice surfaces. Therefore, the application of large-scale satellite remote sensing observations should be investigated, and the spatial validity of dust load snow parameters derived from remote sensing data should be assessed. Kokhanovsky et al. [32] achieved the first step toward this objective by utilizing a high-spectral-resolution Hyperspectral Precursor of the Application Mission or PRecursore IperSpettrale della Missione Applicativa imaging spectroscopy data to retrieve multiple surface snow optical property parameters in the Nansen Ice Shelf and compared them with literature data.

In this study, we validated the accuracy of the dust load satellite retrieval model for snow and ice surfaces by using spectrometer field-measured snow spectral reflectance data. A remote sensing retrieval scheme for extracting dust load parameters from snow and ice surfaces was proposed based on visible infrared imaging radiometer suite (VIIRS)/national polar-orbiting partnership (NPP) surface reflectance daily L2GD 500 m and 1 km (VNP09GA) surface reflectance data and moderate-resolution imaging spectroradiometer (MODIS) Terra/Aqua surface reflectance daily L2G global 500 m and 1 km (MOD09GA) surface reflectance data. In addition, the accuracy of the scheme was evaluated using in situ measurement DMC data.

II. STUDY AREA AND DATA

A. Study Area

In this study, we chose Northeast and Northwest China as study areas to retrieve the dust load on snow surfaces (see Fig. 2). The average elevation in Northeast China (NE) is 443 m, and the study area is located between 121.53° – 130.84° longitude and 43.56° – 48.07° latitude. This region is one of the China's three major winter snow-covered areas. Long-distance cross-border transport of dust is highly susceptible to deposition on snow

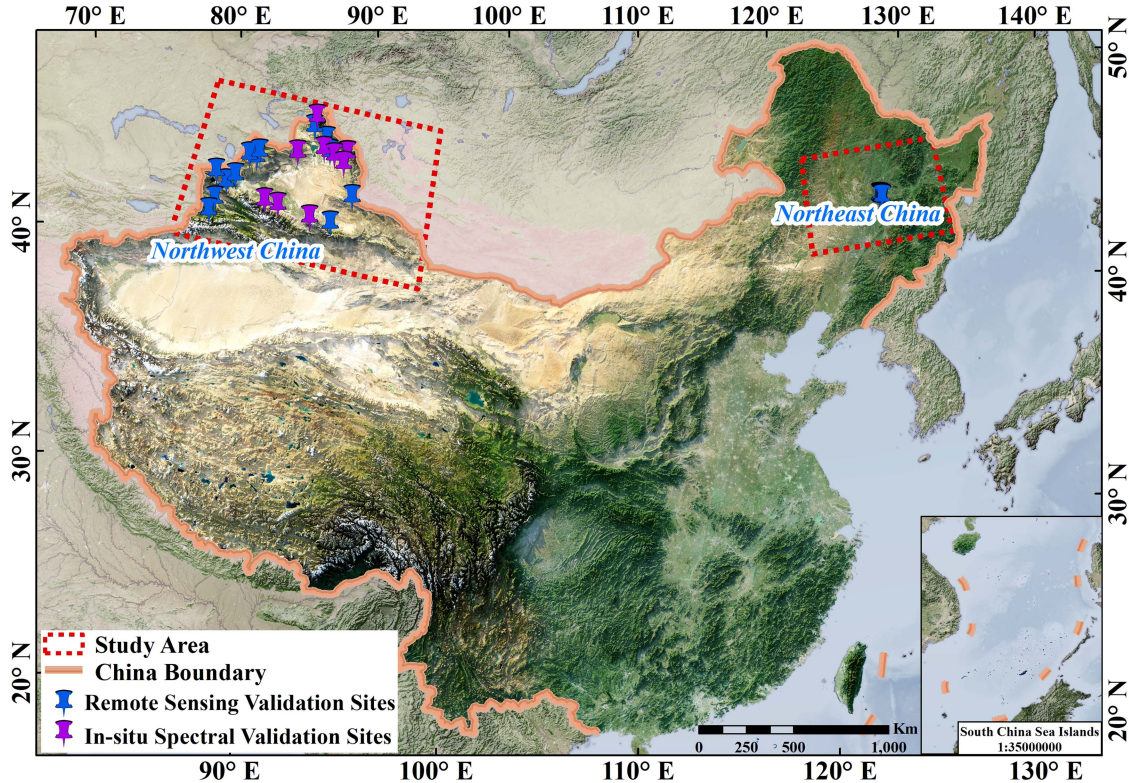


Fig. 2. Overview of the study areas in Northeast and Northwest China (the blue points denote the validation sites for remote sensing retrieval results, the purple points denote the validation sites for in situ spectral reflectance retrieval results, the red dotted lines denote the study areas, and the solid orange line indicates the Chinese national border). The imagery is sourced from the cloud-free results of Sentinel-2 provided by the European Space Agency.

surfaces in this region, affecting snow and ice albedo radiative forcing. The study area in Northwest (NW) China is located north of the Tianshan Mountains at elevations ranging from 154 to 7009 m, and this study area is located between 79.52° – 95.83° longitude and 41.67° – 49.19° latitude. This region exhibits a significant snow cover and numerous snow cover days each year. In this region, dust is the dominant light-absorbing impurity in the snow layer, resulting in changes in snow albedo radiative forcing [12].

B. Data and Preprocessing

1) Remote Sensing Data: In this study, MOD09GA and VNP09GA surface reflectance data are the primary remote sensing data used for DMC retrieval. The top-of-atmosphere reflectance is influenced not only by the reflectance of the underlying polluted snow surface but also by the properties of atmospheric air between the ground and satellite. Both MOD09GA and VNP09GA data are rigorously atmospherically corrected, allowing for large-scale and long time-series monitoring of the snow DMC, and these data achieve excellent performance in retrieving snow optical property parameters [33], [34]. The derivation of MOD09GA and VNP09GA surface reflectance products fully accounts for atmospheric aerosol properties. In addition, it should be noted that the driver data have been atmospherically corrected so that the impact of atmospheric effects is limited and the impact of specific atmospheric correction procedures on retrieval results is reduced.

The channels were selected in such a way that atmospheric gas absorption effects are minimized. We used the 1240 nm channel to determine the snow grain size [31] as large snow grains absorb more light in this channel. Therefore, the snow grain size can be estimated using measurements in this channel with the support of the 865 nm channel [refer to (A11) in Appendix A]. Information on the snow grain size is important for dust load estimation. Further details have been given by Kokhanovsky et al. [31]. The reflectance in the 400 and 490 nm channels is highly influenced by the DMC and dust type (via the dust absorption Ångström exponent).

Based on the above theory and combining the spectral signatures of MOD09GA and VNP09GA data, we determined the optimal retrieval bands ($\lambda_1 = 400$ nm, $\lambda_2 = 490$ nm, $\lambda_3 = 865$ nm, and $\lambda_4 = 1240$ nm) for the dust-loaded snow retrieval model [31]. When using MOD09GA data to retrieve the DMC on snow surfaces, the following bands were selected: sur_refl_b03, sur_refl_b04, sur_refl_b02, and sur_refl_b05. When using VNP09GA data to retrieve the DMC on snow surfaces, the following bands were selected: M1, surface reflectance band M3, surface reflectance band M7, and surface reflectance band M8.

The imaginary part of the ice refractive index needed for bulk ice absorption coefficient $\gamma_i(\lambda)$ calculation was obtained from the existing data [35], [36] (see Table I).

Based on the visual interpretation, it was found that the surface reflectance values of the MOD09GA and VNP09GA data are similar in bands sur_refl_b03 and M1, sur_refl_b04 and M3, and

TABLE I
IMAGINARY PART OF THE ICE REFRACTIVE INDEX FOR THE DMC RETRIEVAL BAND

Bands used in the retrieval model	MOD09GA	Imaginary part of the ice refractive index	VNP09GA	Imaginary part of the ice refractive index
λ_1 (400 nm)	sur_refl_b03 (459–479 nm)	6.2751×10^{-10}	band M1 (402–422 nm)	2.669×10^{-11}
λ_2 (490 nm)	sur_refl_b04 (545–565 nm)	1.0791×10^{-9}	band M3 (478–488 nm)	2.861×10^{-10}
λ_3 (865 nm)	sur_refl_b02 (841–876 nm)	2.150×10^{-7}	band M7 (846–885 nm)	2.150×10^{-7}
λ_4 (1240 nm)	sur_refl_b05 (1230–1250 nm)	1.220×10^{-5}	band M8 (1230–1250 nm)	1.220×10^{-5}

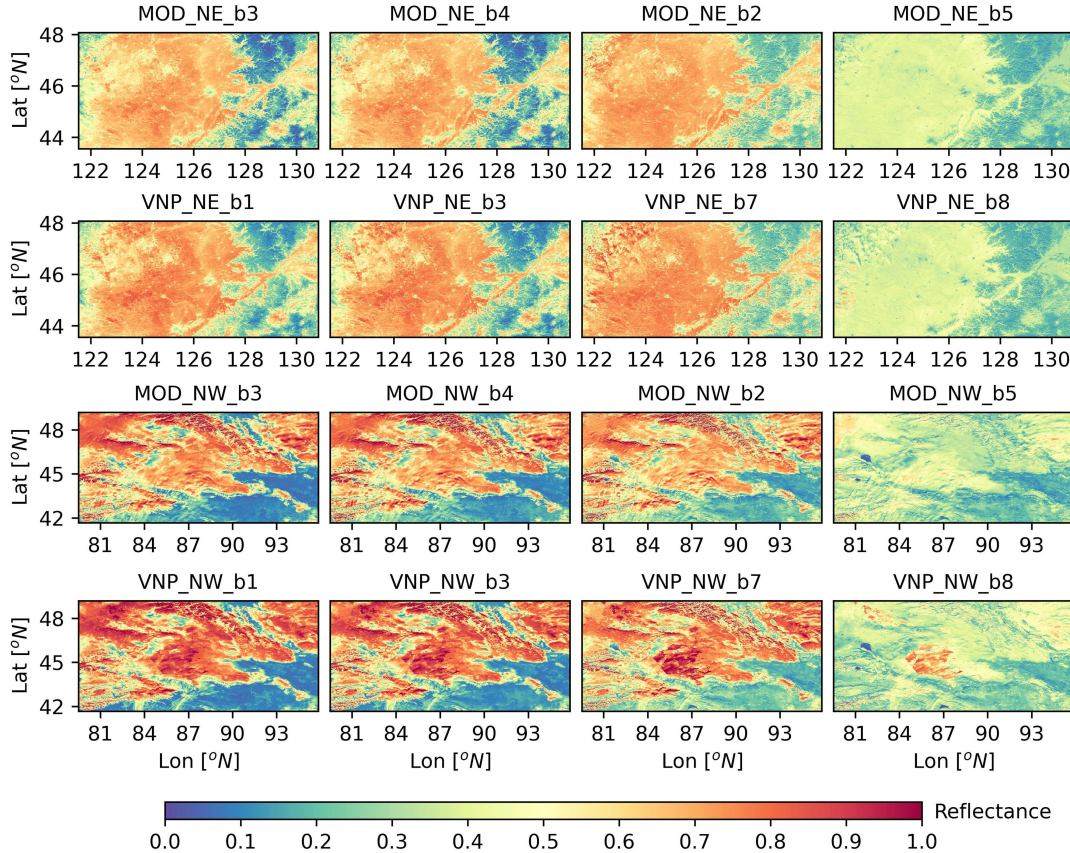


Fig. 3. Reflectance differences between the four MODIS channels (bands 3, 4, 2, and 5) and VIIRS channels (bands 1, 3, 7, and 8) used for dust-loaded snow retrieval. The symbols “MOD_NE” and “MOD_NW” represent the surface reflectance of MOD09GA data in Northeast and Northwest China, respectively. Similarly, the symbols “VNP_NE” and “VNP_NW” represent the surface reflectance of VNP09GA data in Northeast and Northwest China, respectively. NE (Date: 15 January 2020) and NW (Date: 5 January 2020).

sur_refl_b02 and M7, and the values almost completely overlap in bands sur_refl_b05 and M8 (see Fig. 3). With the use of both datasets to retrieve the DMC in snow, we could compare them and improve the reliability of the retrieval results. In addition, the use of multiple satellite products could allow us to assess the

impacts of the remote sensing spectral data range and bandwidth on DMC retrieval from snow layers.

Although the reflectance values in the above four bands are similar, there are slight differences. These differences can be attributed to four factors:

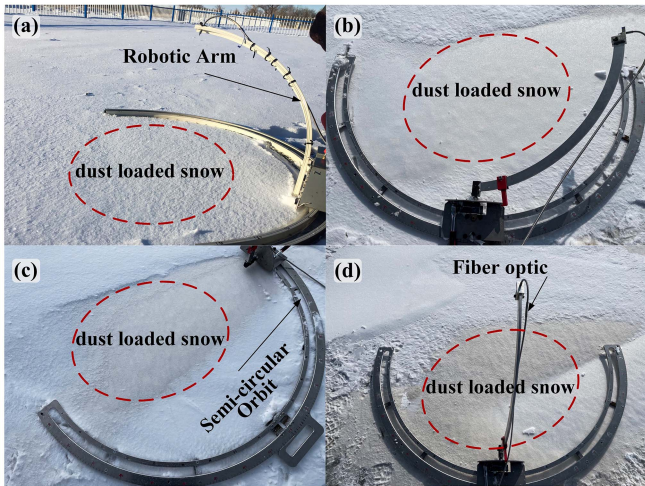


Fig. 4. BRDF measuring instrument. (a)–(d) Each shows a multiangle observation of the dust-loaded snow reflectance at different levels of dust pollution.

- 1) the different spectral response functions of the sensors for obtaining MOD09GA and VNP09GA data;
- 2) different calibration processes of the sensors for obtaining MOD09GA and VNP09GA data;
- 3) different bandwidths of similar bands for MOD09GA and VNP09GA data;
- 4) different processing algorithms for MOD09GA and VNP09GA data.

In the model retrieval process, MODIS/Terra snow cover daily L3 global 500 m SIN grid (MOD10A1 SCD version 6) data were used to identify snow-covered areas based on the MOD09GA bands, while VIIRS/NPP snow cover daily L3 global 375 m SIN grid (VNP10A1 SCD version 6) data were used for the VNP09GA bands.

2) Field Observation Data:

a) DMC measurements: DMC measurements are typically conducted in a laboratory setting, necessitating snow cover sampling. The sampling specifications adhered to the principles delineated by Wang et al. [37]. With the use of disposable gloves, a snow shovel was employed to collect snow samples from the top of the snow surface (< 2 cm), which were then compacted and sealed in 2-L Whirl-Pak bags, with each snow sample bag numbered. Each observation involved multiple samplings to avoid accidental errors. The snow samples were frozen until they were returned to the laboratory for DMC measurement. In addition, the coordinates, time, temperature, and snow depth were recorded.

The snow and ice samples collected in the field were transported in a frozen state to the laboratory. After the snow and ice samples had completely melted at room temperature, they were filtered through quartz filters (Whatman QMA) and combusted in a muffle furnace at 600 °C for 6 h. The quartz filters were placed in an ultraclean drying oven at 60 °C for 24 h. After complete drying, they were weighed using a microbalance with an accuracy of 0.1 mg. The dust content in snow and ice was defined as the mass difference between the quartz filters before and after sample filtering divided by the volume of the filtered snowmelt

sample. Strict data quality control was performed in this study, which excluded potential errors, such as transient clouds and improper storage of the snow samples, and ensured the validity of all data. In the Northwest China study area (measurement period: 15–25 January 2016, and 23 November 2016–23 March 2017), we obtained 13 observation groups (the observation groups refer to data records that include the observation coordinates, time, DMC, and spectrum. The data not only include the DMC but also include other auxiliary data. Hence, we referred to these data as observation groups in this study) of valid measured DMC data for snow and ice surfaces. In Northeast China (measurement period: 24 December 2018 to 24 February 2019), we obtained 12 observation groups of valid measured DMC data for snow and ice surfaces. All field-observed DMC samples were acquired based on the satellite transit time measurements.

Potential errors due to scale effects between point-by-point observations and satellite retrievals were considered in this study. In the field observations, 500 m × 500 m samples were selected for validation, and each sample was divided into 10 × 10 subgrid samples. The average dust content in all subgrid samples approximately represents the dust content information of a single-point snow and ice surface on a 500 m scale.

b) In situ snow spectral reflectance measurements: Given the potential impacts of snow as a typical forward scattering medium and the satellite imaging azimuth on the retrieval results, it is inadequate to exclusively rely on the spectra procured from nadir-directed observations to validate the precision of DMC retrieval based on the dust-loaded snow retrieval model. Consequently, we used a snow bidirectional reflectance distribution function (BRDF) observation instrument to conduct several field surveys and comprehensively verified the accuracy of the DMC retrieval algorithm.

The reflectance measurement entailed the application of the PSR-3500 field spectroradiometer, which is a SPECTRAL EVOLUTION, Inc., product with an observational bandwidth spanning 350–2500 nm. This instrument offers a spectral resolution of 1 nm with a 25° field-of-view fiber optic cable. The PSR-3500 spectrometer can achieve data acquisition within the full spectral range in 100 ms, reaching a scan rate of 10 times/s. The mean of ten spectra was preserved as the actual spectrum acquired. A multiangle reflectance instrument was installed to observe the dust-loaded snow reflectance within the range of viewing zenith angles of 0°, 10°, 20°, 30°, 40°, 50°, and 60° (see Fig. 4). The solar zenith angle was calculated from the measurement point longitude, latitude, and time. In this study, we measured the in situ snow spectral reflectance for 12 groups to calculate the DMC, and 12 groups of the DMC corresponding to the in situ snow spectral reflectance were additionally measured.

III. METHODS

Here, we introduce a new method based on the well-established ART theory combined with remote sensing data for monitoring the dust load on snow surfaces. The new method combines the advantages of satellite remote sensing for spatial and temporal monitoring on a large scale. We extend the dust-loaded snow retrieval model from a single point to a larger spatial

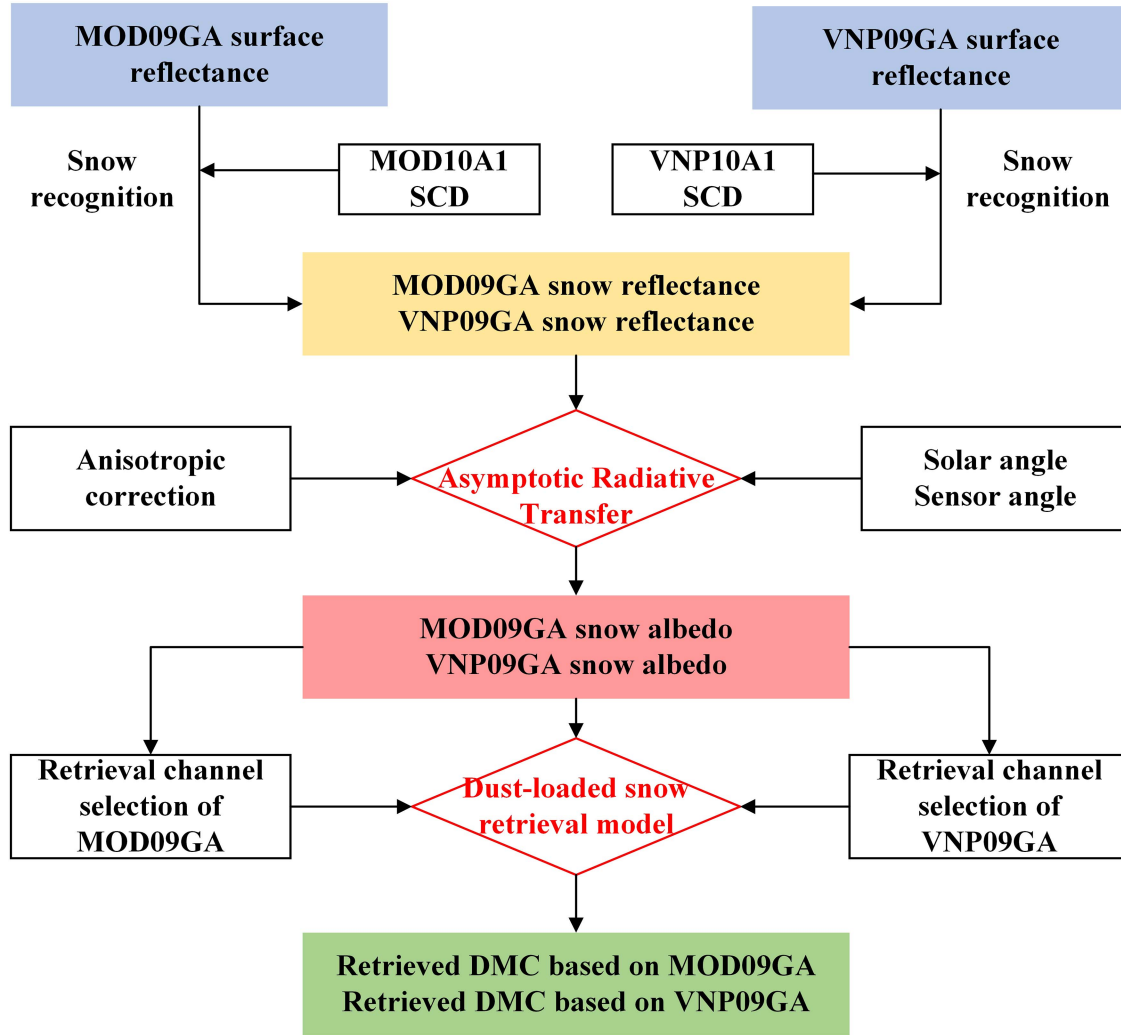


Fig. 5. General flow of DMC retrieval from the remotely sensed spectral reflectance.

scale. This permits the dust-loaded snow retrieval model to simulate DMCs in snow and ice. This research is crucial for directly monitoring spatiotemporally distributed snow and ice surface dust loads by utilizing satellite remote sensing observations.

In this study, the snow and ice DMC retrieval scheme considering near-real-time retrievals is based on the ART theory proposed by Kokhanovsky and Zege [38] (refer to Appendix A), and it was used to obtain the spatiotemporal distribution of the snow and ice DMC in Northwest and Northeast China [31], [39]. The technique proposed by Kokhanovsky et al. [31] relating the snow reflectance and dust load in snow is based on the full physics approach and does not rely on the established correlations between the reflectance and dust load. This approach comprehensively considers the observation geometry [31], [32]. The retrieval technique is based on the principle that the snow reflectance decreases with wavelength in the visible range in the case of polluted snow, while the reflectance remains almost constant in the visible range in the case of clean snow surfaces. The snow reflectance decline in the visible region is greater for high dust concentrations. In this article, we first validated

the algorithm against in situ observations. In this theory, the spherical albedo r_s of dust-loaded snow can be obtained with (1) (the specific physical meaning is detailed in Appendix A)

$$r_s = \exp \left\{ -\sqrt{ML} \right\} \quad (1)$$

where L is the effective absorption length (EAL) and M is an intermediate variable.

The DMC c_m of dust-loaded snow can be obtained as follows:

$$c_m = \frac{\rho_d}{\rho_i} \frac{c_{\text{pol}}}{c_{\text{ice}}} \quad (2)$$

where ρ_d is the dust density and ρ_i is the ice density. Generally, $\rho_d = 2.65 \text{ g/cm}^3$ and $\rho_i = 0.917 \text{ g/cm}^3$. Moreover, c_{ice} is the volumetric concentration of ice grains in snow, and c_{pol} is the volumetric concentration of dust in the snowpack. The detailed theoretical method and derivation process of the retrieval equations for dust load retrieval are provided in Appendix A. The general flow of the DMC retrieval process based on MOD09GA and VNP09GA surface reflectance data is shown in Fig. 5. The DMC retrieval process mainly includes three aspects: first,

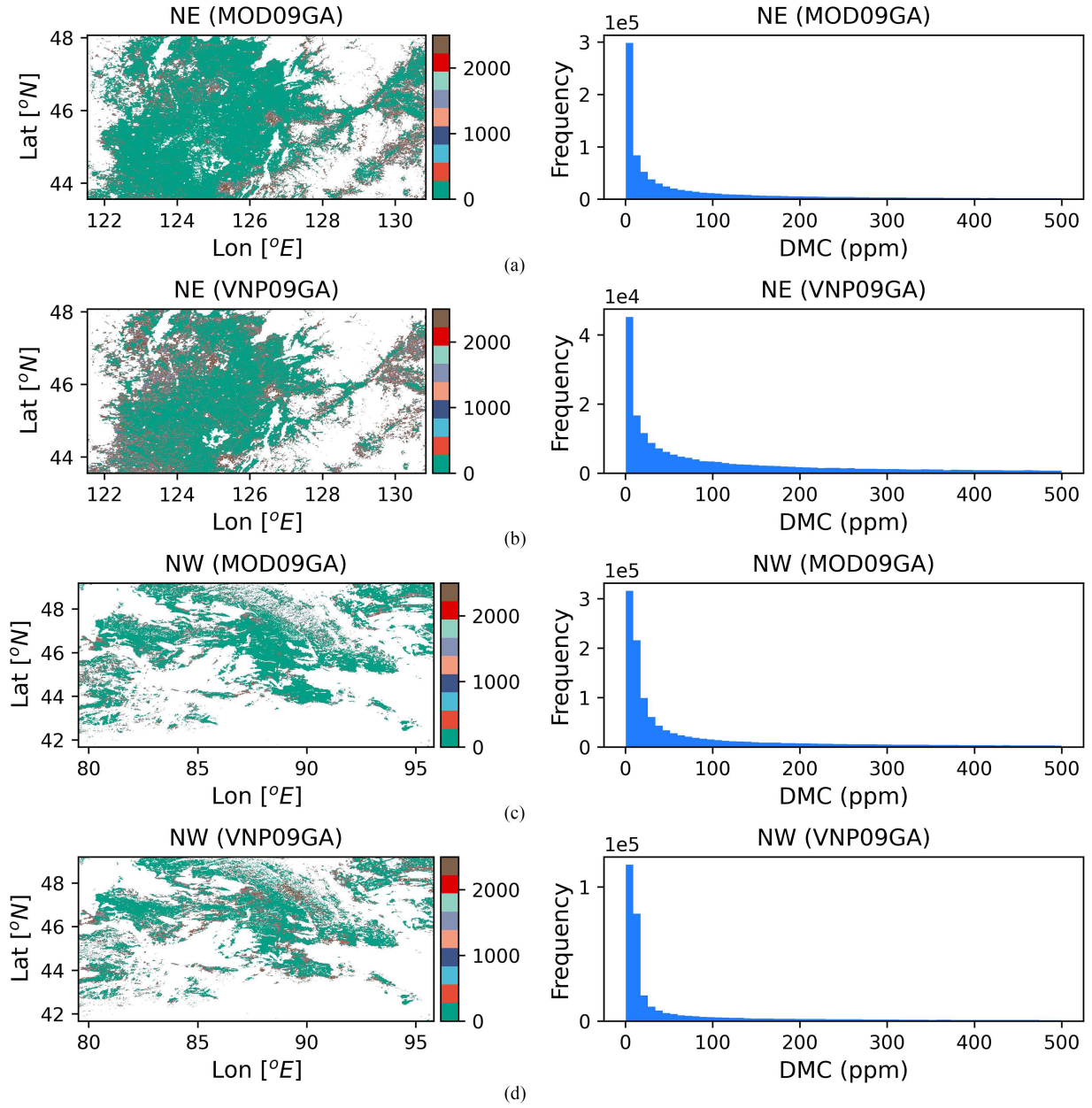


Fig. 6. Snow surface DMC retrieval results. (a) Shows the retrieved DMC based on MOD09GA data in the Northeast China region (unit: ppm; date: 15 January 2020). (b) Shows the retrieved DMC based on VNP09GA data in the Northeast China region (unit: ppm; date: 15 January 2020). (c) Shows the retrieved DMC based on MOD09GA data in the Northwest China region (unit: ppm; date: 5 January 2020). (d) Shows the retrieved DMC based on VNP09GA data in the Northwest China region (unit: ppm; date: 5 January 2020).

MOD10A1 SCD and VNP10A1 SCD data were employed to obtain MOD09GA and VNP09GA snow reflectance values; second, the ART model was utilized to retrieve MOD09GA and VNP09GA snow albedo values; and third, the dust-loaded snow retrieval model was used to retrieve the DMC in snow.

In this study, we used the mean absolute error (MAE), root-mean-square error (RMSE), Pearson's correlation coefficient (R), coefficient of determination (R^2), and coefficient of variation (CV) to assess the accuracy of the dust-loaded snow retrieval model. The definitions of the MAE, RMSE, R , R^2 , and CV are detailed in Appendix B.

The MAE provides a straightforward interpretation of the average prediction error of the dust-loaded snow retrieval model, while the RMSE indicates the overall accuracy and the impact of larger errors in the dust-loaded snow retrieval model. R indicates the degree of association between the retrieved and observed DMC values, while R^2 indicates the snow ability of the dust load retrieval model to simulate the variance in the DMC. The CV allows for comparing the consistency and reliability between the retrieved DMC from the in situ spectral reflectance and the in situ measured DMC, thereby evaluating the stability of the simulation outputs of the dust-loaded snow retrieval model.

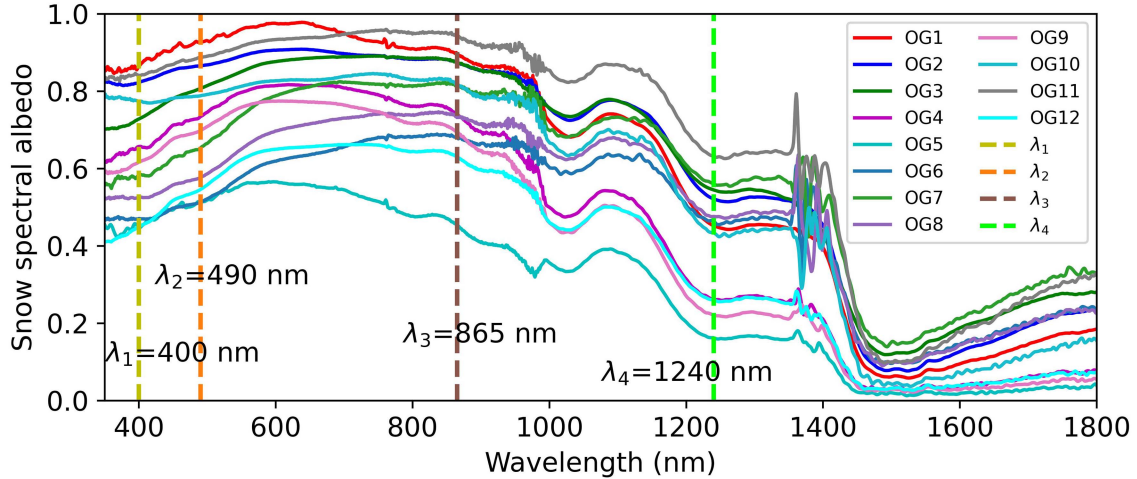


Fig. 7. Spectral reflectance of dust-covered snow observed by the spectrometer in the field. OG1–OG12 indicate the observation group snow spectral reflectance values at different DMC levels. The characteristic wavelengths used for snow and ice surface dust load retrieval are $\lambda_1 = 400$ nm, $\lambda_2 = 490$ nm, $\lambda_3 = 865$ nm, and $\lambda_4 = 1240$ nm (see Appendix A).

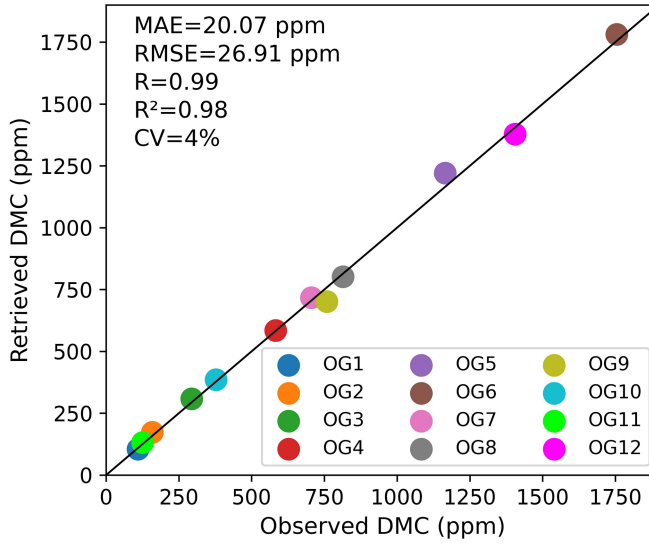


Fig. 8. Comparison of the in situ DMC and those DMC retrieved from the in situ spectral reflectance (OG1–OG12 indicate the observation group).

IV. RESULTS

A. Retrieval of the DMC Based on the Remotely Sensed Snow Spectral Reflectance

In this study, we retrieved the DMC in two regions, i.e., Northwest China (date: 5 January 2020) and Northeast China (date: 15 January 2020), using MOD09GA and VNP09GA surface reflectance data, respectively (see Fig. 6).

The spatial retrieval results showed that the DMC on snow and ice surfaces retrieved by the model ranges from 0 to 2500 ppm. In fact, in most regions of Northwest China and Northeast China, the DMC on snow and ice surfaces is below 500 ppm, and only a few regions exhibit DMC values above 500 ppm. In Northeast China, the average DMC retrieved by using the MOD09GA (VNP09GA) surface reflectance data in January was 138.18 ppm (253.81 ppm) [see Fig. 6(a) and (b)].

In Northwest China, the average DMC retrieved by using the MOD09GA (VNP09GA) surface reflectance data in this region in January was 43.59 ppm (45.30 ppm) [see Fig. 6(c) and (d)]. In addition, studies based on manual field observations in the same areas have revealed that the average DMC on snow and ice surfaces in Northwest China is 17.3 ± 38.1 ppm [12]. In the urban regions of Northeast China, the average DMC on snow and ice surfaces in January is 223.83 ppm [13]. Therefore, the DMC retrieved from remote sensing data can reflect the spatial distribution characteristics of the natural dust content on snow and ice surfaces. Although the DMC values retrieved by using the VNP09GA and MOD09GA surface reflectance data exhibited similar distribution characteristics, differences occurred in local areas. In general, the different sensors using the new retrieval method could obtain the same DMC accuracy. The main reason for the DMC retrieval accuracy difference here is the notable difference in the reflectance used for DMC retrieval between the MOD09GA and VNP09GA data (see Fig. 3). The dust-loaded snow retrieval model employed in this study is based on the spectral reflectance to retrieve the dust content on snow surfaces. Therefore, the retrieval results are influenced by the magnitude of the reflectance. When extending this method to satellite remote sensing data retrieval, the input data for the retrieval model becomes the narrow-band reflectance. Because the MOD09GA and VNP09GA narrow-band reflectance values differ, the retrieval results vary. The difference in the retrieval results based on different narrow-band reflectance inputs does not necessarily suggest a lack of accuracy in the retrieval algorithm. In contrast, this precisely highlights the sensitivity of the retrieval model to the input data characteristics.

B. Comparison of the In Situ DMC to the DMC Retrieved From the In Situ Spectral Reflectance and the Remotely Sensed Retrieved DMC

In general, dust more significantly impacts the snow spectral reflectance in the visible band in most of the cases, while it

TABLE II
PARAMETERS OF THE RETRIEVED DUST-LOADED SNOW UTILIZING THE IN SITU SNOW SPECTRAL REFLECTANCE

Observation group (OG)	Ångström absorption exponent	Dust mass absorption coefficient (m^2/g)	Dust grain size (μm)	DMC (ppm)
OG1	3.34	3.78×10^{-3}	6.23	105.05
OG2	3.57	3.93×10^{-3}	8.04	172.79
OG3	4.18	4.42×10^{-3}	4.74	308.46
OG4	2.78	3.52×10^{-3}	13.22	584.62
OG5	3.10	3.65×10^{-3}	11.02	1220.59
OG6	1.70	3.37×10^{-3}	21.98	1781.54
OG7	4.34	3.83×10^{-3}	8.88	716.73
OG8	2.16	3.38×10^{-3}	17.97	801.79
OG9	3.94	4.21×10^{-3}	5.90	701.10
OG10	1.63	3.38×10^{-3}	22.65	385.51
OG11	1.02	17.51×10^{-3}	4.92	131.70
OG12	3.28	3.75×10^{-3}	9.77	1377.62

imposes a negligible effect on the snow spectral reflectance in the near-infrared band in most cases. Regarding dust deposited on snow and ice surfaces, the DMC and dust grain size directly affect the variation in the snow spectral reflectance (see Fig. 7).

Based on the in situ snow spectral reflectance, we retrieved the DMC and other parameters for dust-loaded snow (see Table II). This represents an effective method for the quantitative retrieval of various intrinsic physical properties of snow based on in situ snow spectral reflectance data.

The MAE, RMSE, R , R^2 , and CV values between the observed and retrieved DMC values were 20.07 ppm, 26.91 ppm, 0.99, 0.98, and 4%, respectively (see Fig. 8). DMC retrieval from the in situ spectral reflectance achieved a high degree of accuracy. The retrieval error increased when retrieving the DMC from snow and ice surfaces with a very high dust content. This possibly occurs because the model ignores light scattering by dust grains in snow.

To further evaluate the difference between the DMC retrieved from the in situ spectral reflectance and the remotely sensed retrieved DMC, we used in situ measurement DMC data for Northeast and Northwest China to verify the accuracy of DMC retrieval from remotely sensed spectral reflectance data (see Fig. 9 and Fig. 10, respectively).

In Northwest China, the MAE and RMSE of the DMC values retrieved by utilizing the VNP09GA data were 8.66 ppm and 9.78 ppm, respectively, and the MAE and RMSE of the DMC values retrieved by utilizing the MOD09GA data were

11.64 ppm and 13.74 ppm, respectively. In Northeast China, the MAE and RMSE of the DMC values retrieved by utilizing the VNP09GA data were 59.18 ppm and 73.98 ppm, respectively, and the MAE and RMSE of the DMC values retrieved by utilizing the MOD09GA data were 123.28 ppm and 184.32 ppm, respectively. Overall, the accuracy of DMC retrieval by utilizing the VNP09GA data was higher than that utilizing the MOD09GA data. There is a significant difference in DMC retrieval accuracy between the Northeast China and Northwest China. The retrieval accuracy in Northwest China is higher than those in the Northeast China region, regardless of whether MOD09GA data or VNP09GA data are used.

The comparison to in situ DMC measurements (which can be considered the ground truth) revealed that the accuracy of DMC retrieval from the in situ spectral reflectance is much higher than that of DMC retrieval from remotely sensed spectral reflectance data (see Figs. 8 and 9). The reasons are as follows: the wavelength interval of the in situ measurement spectral reflectance is narrower than that of the remotely sensed spectral reflectance. Therefore, when retrieving the DMC in snow based on in situ measurements of the spectral reflectance, the fine change characteristics of the DMC can be more accurately captured. There is almost no scale effect when comparing the in situ DMC measurements to the DMC retrieval results from the in situ spectral reflectance. In contrast, when comparing the in situ DMC measurements to the DMC retrieval results from the remotely sensed spectral reflectance data, scale differences

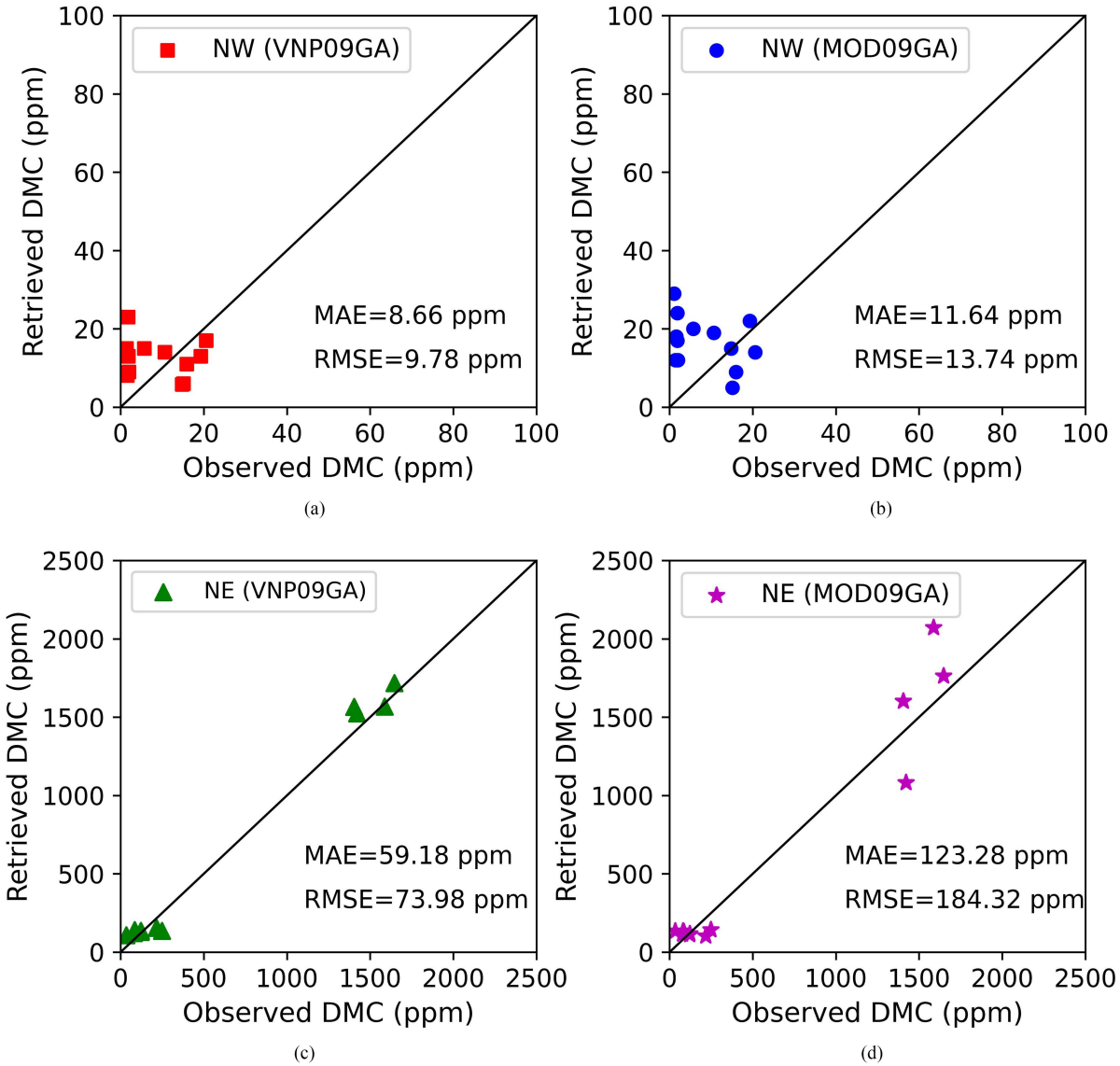


Fig. 9. Evaluation of the accuracy of the retrieved DMC versus the observed DMC. (a) and (b) Show the verification results of the retrieved DMC based on VNP09GA and MOD09GA data, respectively, in Northwest China. (c) and (d) Show the verification results of the retrieved DMC based on VNP09GA and MOD09GA data, respectively, in Northeast China.

were observed. This is also an important reason why the retrieved DMC from the in situ spectral reflectance is closer to the in situ measured DMC. In situ measurements of the spectral reflectance are not subject to atmospheric effects. Although atmospheric effects slightly impact remotely sensed observations at high altitudes, both the VNP09GA and MOD09GA surface reflectance data have been subjected to atmospheric correction. However, the atmospheric effects are clearly greater on the remotely sensed spectral reflectance than on the in situ measurement spectral reflectance.

V. DISCUSSION

A. Advantages and Limitations of Remote Sensing Retrieval of Dust-Loaded Snow

Although the accuracy of manual observations of the DMC on snow and ice surfaces is high, the timeliness and spatial

range are limited [14]. The accuracy of snow and ice surface DMC data simulated by climate models based on emission inventories is poor [40]. In contrast, DMC retrieval from remotely sensed spectral reflectance data provides the advantages of high accuracy, notable timeliness, and wide spatial coverage. The relative deviation between the DMC estimated by the coupled regional climate model (RegCM-4.6.0) and community land model (CLM4.5) and the measured DMC varies between 33% and 100% [41]. In our study, the relative deviation between the snow surface DMC retrieved based on the satellite remote sensing data and the measured DMC varied between 28% and 78%, and the accuracy is higher than that of the integrated model results of the RegCM-4.6.0 and CLM4.5 models. In fact, in the estimation of the snow surface DMC, the WRF-Chem model is utilized in most studies. DMC data for the snow layer estimated based on the WRF-Chem model have been widely used in studies related to radiative forcing [8]. However, existing research has

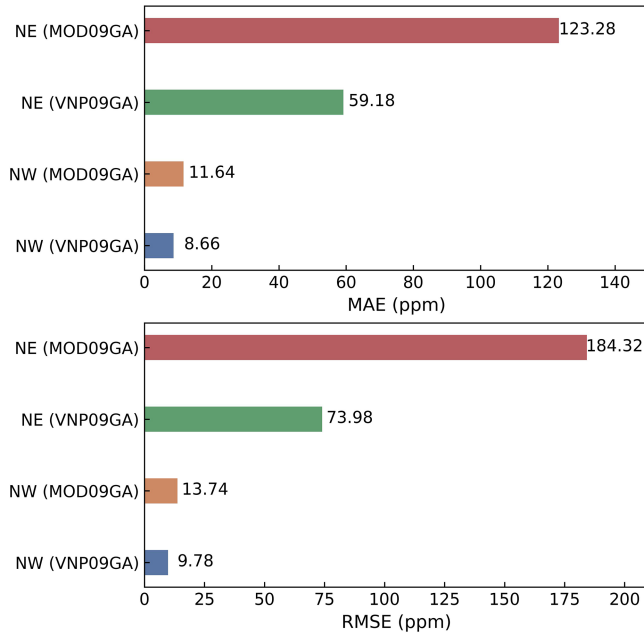


Fig. 10. Accuracy comparison of the DMC values retrieved by using remote sensing data. NW (VNP09GA) denotes the Northwest China (VNP09GA), NW (MOD09GA) denotes the Northwest China (MOD09GA), NE (VNP09GA) denotes the Northeast China (VNP09GA), and NE (MOD09GA) denotes the Northeast China (MOD09GA).

indicated that the WRF-Chem model underestimates the dust deposition flux by 63% relative to observations [42]. In the Himalayan ranges, the DMC estimated based on the WRF-Chem model deviates by one order of magnitude (1000 ppm) from the measured DMC [43]. In our study, the maximum deviation of the DMC values retrieved based on the dust-loaded snow retrieval model in Northeast China reached 483.50 ppm (see Fig. 9). The precision of DMC retrieval based on the dust-loaded snow retrieval model was also higher than that of the WRF-Chem model.

Although the in situ snow spectral reflectance was used to retrieve the DMC, the MAE is 20.07 ppm. However, the retrieval results based on remotely sensed spectral reflectance data are still not comparable to those based on the in situ snow spectral reflectance, in which the average MAE of the DMC values retrieved by using the VNP09GA data is 33.92 ppm and that of the values retrieved by using the MOD09GA data is 67.46 ppm. The accuracy of remotely sensed spectral reflectance retrieval is significantly lower than that based on the in situ snow spectral reflectance. In conclusion, the current margin of error of the retrieval results is acceptable. However, there remain certain problems with the proposed retrieval method. For example, the universality in different regions must be improved, and the retrieval bands and parameters should be adjusted according to the snow characteristics of other areas.

B. Challenges of This Study

The remaining challenges of this study are mainly reflected in the following aspects.

- 1) When dust on the surface of old snow is covered by new snowfall, the manual sampling method can be employed to obtain the natural DMC. However, since the penetration degree of optical remote sensing systems is limited, the snow spectral reflectance observed by optical remote sensing does not capture the actual characteristics that change after the surface is covered by snow. The above phenomenon is also the main reason for the low accuracy of remote sensing retrieval relative to the single-point scale.
 - 2) The DMC values obtained by different experimental measurement instruments when processing snow and ice samples containing dust vary greatly [16]. Therefore, the in situ observed DMC can hardly represent the real DMC in snow. In this case, when using the in situ observed DMC to evaluate the remotely sensed retrieved DMC, the quality of the remote sensing retrieval results cannot be ensured.
 - 3) In this study, to construct a simple semiphysical retrieval model of snow and dust properties, spatially uniform distribution characteristics of dust on snow and ice surfaces were assumed [31], [44]. However, the distribution of dust on snow and ice surfaces is often highly heterogeneous under natural conditions, which is another crucial factor contributing to the limitations of the model. In regard to nonuniform dust-loaded snow, this assumption is not favorable to the retrieval of the true snow surface DMC.
 - 4) In addition, the complex terrain and issues of scale between in situ measurements and satellite remote sensing observations introduce uncertainty that affects the inter-comparison of the in situ observed DMC and the remotely sensed retrieved DMC.
 - 5) There are still potential errors in mutual verification between single-point observations and satellite pixels. More in situ DMC data or a well-developed scale conversion scheme could further reduce this uncertainty.
- When the dust-loaded snow retrieval model is applied to remote sensing observations, the following methods could improve the model retrieval accuracy and provide more meaningful validation.
- 1) The atmospheric correction methods of MODIS and VI-IRS data should be improved, and an atmospheric correction algorithm suitable for snow-covered surfaces should be developed.
 - 2) The influence of the characteristics of complex terrain, including the slope and direction of observation, should be considered in the retrieval model.
 - 3) In the dust-loaded snow retrieval model, the homogeneity of the dust distribution along the horizontal and vertical directions in the snowpack should be considered.
 - 4) More careful in situ DMC measurements should be performed involving 500 m satellite pixels by increasing the number of measurement points.

VI. CONCLUSION

In this study, we applied a rapid retrieval scheme for measuring dust on snow and ice surfaces based on the optical

characteristic parameters derived from remote sensing data using ART theory. With this new scheme, it was possible to retrieve DMC data over larger spatial domains.

Our results suggested that the accuracy of DMC retrieval from the in situ spectral reflectance is higher than that from remotely sensed spectral reflectance data. The retrieved DMC based on the in situ snow spectral reflectance is highly accurate, and the RMSE is 26.91 ppm. The accuracy of dust load retrieval by using the VNP09GA surface reflectance data is higher than that by using the MOD09GA surface reflectance data. In Northwest China, the RMSE of the DMC values retrieved by using the VNP09GA surface reflectance data is 3.96 ppm smaller than that of the values retrieved by using the MOD09GA surface reflectance data. In Northeast China, the RMSE of the DMC values retrieved from the VNP09GA surface reflectance data is 110.34 ppm smaller than that of the values retrieved from the MOD09GA surface reflectance data.

We identified a basic retrieval rule indicating that the data with higher spectral resolution could provide a higher DMC retrieval accuracy. Moreover, both the band range and bandwidth of the remotely sensed spectral reflectance data affected the DMC retrieval accuracy. Although high spectral resolution in situ spectral measurement data could yield more accurate DMC values, they are unsuitable for monitoring snow and ice surface dust load information on a large spatial scale for long time series.

This study contributes to the large-scale monitoring of the dust load on snow and ice surfaces, which is critical for further explorations of how dust affects the snow and ice albedo. It is foreseeable that high-precision estimation of snow surface dust content on such a large scale will certainly facilitate quantitative studies on the effects of light-absorbing impurities on snow and ice melting and snow and ice water resources.

APPENDIX

A. THEORETICAL MODEL FOR DUST LOAD RETRIEVAL FROM SNOW SURFACES

We used the following analytical model to determine the solar light reflectance R_s for a snow layer covered in dust [31], [38], [39]

$$R_s(\mu, \mu_0, \psi) = R_0(\mu, \mu_0, \psi) r_s^\xi \quad (\text{A1})$$

where

$$\xi = \frac{u(\mu_0) u(\mu)}{R_0(\mu, \mu_0, \psi)} \quad (\text{A2})$$

$$u(\mu_0) = \frac{3}{5} \mu_0 + \frac{1 + \sqrt{\mu_0}}{3} \quad (\text{A3})$$

$$r_s = \exp \left\{ -\sqrt{ML} \right\} \quad (\text{A4})$$

where

$$M = \gamma_i(\lambda) + \beta(\lambda/\lambda_0)^{-\alpha} \quad (\text{A5})$$

$$\beta = ck_0 B^{-1} \quad (\text{A6})$$

where μ_0 is the solar zenith angle, μ is the sensor zenith angle, and ψ is the relative azimuth angle. Moreover, $\gamma_i(\lambda)$ is the bulk ice absorption coefficient, L is the EAL, c is the relative pollutant volumetric concentration, B is the absorption enhancement

parameter (set to 1.8), k_0 is the volumetric absorption coefficient of dust particles at wavelength λ_0 , and R_0 is the reflectance of the nonabsorbing snow layer. Notably, R_s depends on four unknown parameters: R_0 , L , α , and β . These parameters do not depend on the wavelength and can be derived from spectral measurements of the reflectance R_s . In particular, the function can be minimized as follows:

$$F(\lambda) = \|R_{\text{meas}}(\lambda) - R_s(\lambda)\|^2. \quad (\text{A7})$$

The above can be performed to obtain all four parameters. In this work, we used the approximate analytical solution of this retrieval problem suggested by Kokhanovsky et al. [31], [39] using measurements at four wavelengths, namely, $\lambda_1 = 400$ nm, $\lambda_2 = 490$ nm, $\lambda_3 = 865$ nm, and $\lambda_4 = 1240$ nm

$$\alpha = \frac{2 \ln z}{\ln(\lambda_2/\lambda_1)} \quad (\text{A8})$$

$$z = \ln r_{s,\lambda_1} / \ln r_{s,\lambda_2} \quad (\text{A9})$$

$$L = \frac{\ln^2 r_s(\lambda_3)}{\gamma_i(\lambda_3)} \quad (\text{A10})$$

$$R_0 = R_3^\varepsilon R_4^{1-\varepsilon}, \varepsilon = 1/(1-\varsigma), \varsigma = \sqrt{\gamma_3/\gamma_4} \quad (\text{A11})$$

$$\beta = \left(\frac{\lambda_1}{\lambda_0} \right)^\alpha \ln^2 r_{s1}. \quad (\text{A12})$$

The value of β can be used to obtain the dust load

$$c_m = \frac{B \rho_d}{k_0 \rho_i} \beta. \quad (\text{A13})$$

The values of k_0 (mm⁻¹) and B were assumed. k_0 is taken at the wavelength $\lambda_0=1\mu\text{m}$. We adopted the following approximate relationship between k_0 and α [31]:

$$k_0 = \sum_{i=0}^2 b_i \alpha^i = b_0 \alpha^0 + b_1 \alpha^1 + b_2 \alpha^2 \quad (\text{A14})$$

where α is the impurity Ångström absorption exponent. We assumed the density of dust ($\rho_d = 2.65 \text{ g/cm}^3$), the density of ice ($\rho_i = 0.917 \text{ g/cm}^3$), $b_0 = 10.916$, $b_1 = -2.0831$, and $b_2 = 0.5441$.

The size of ice grains can be determined as follows:

$$d = L/16. \quad (\text{A15})$$

The size of dust particles d_{ef} (μm) can be estimated as follows:

$$d_{ef} = \sum_{i=0}^2 h_i \alpha^i = h_0 \alpha^0 + h_1 \alpha^1 + h_2 \alpha^2 \quad (\text{A16})$$

where $h_0 = 39.7373$, $h_1 = -11.8195$, and $h_2 = 0.8235$.

The technique specified above can be used for the interpretation of the in situ spectral reflectance. In the case of satellite measurements, atmospheric correction must be performed. The theory we use is valid only for dry snow. So, the temperatures must be below zero. The main parameters influencing snow spectral reflectance are grain size and impurity load. In this study, we employed widely used land surface reflectance remote sensing products (MOD09GA and VNP09GA), which have been atmospherically corrected, to directly retrieve the dust load on snow surfaces.

B. DEFINITION OF THE MAE, RMSE, R, R², AND CV

$$\text{MAE} = \frac{1}{n} \sum_{i=1}^n |f_i - y_i| \quad (\text{B1})$$

$$\text{RMSE} = \left[\frac{\sum_{i=1}^n (f_i - y_i)^2}{n} \right]^{\frac{1}{2}} \quad (\text{B2})$$

$$R = \frac{1}{n-1} \sum_{i=1}^n \left(\frac{f_i - \bar{f}}{\sigma_f} \right) \left(\frac{y_i - \bar{y}}{\sigma_y} \right) \quad (\text{B3})$$

$$R^2 = \frac{\sum_{i=1}^n (f_i - \bar{y})^2}{\sum_{i=1}^n (y_i - \bar{y})^2} \quad (\text{B4})$$

$$\text{CV} = \frac{\text{RMSE}}{\bar{f}} \quad (\text{B5})$$

where n is the number of measurement samples in the validation data, f_i denotes the retrieval results of the dust-loaded snow retrieval model, and y_i denotes the measured results. \bar{f} and \bar{y} are the averages of the retrieved and measured results, respectively, and σ_f and σ_y are the standard deviations of the retrieved and measured results, respectively.

REFERENCES

- [1] N. M. Mahowald et al., "Observed 20th century desert dust variability: Impact on climate and biogeochemistry," *Atmos. Chem. Phys.*, vol. 10, no. 22, pp. 10875–10893, 2010, doi: [10.5194/acp-10-10875-2010](https://doi.org/10.5194/acp-10-10875-2010).
- [2] B. Di Mauro et al., "Mineral dust impact on snow radiative properties in the European Alps combining ground, UAV, and satellite observations," *J. Geophys. Res., Atmos.*, vol. 120, no. 12, pp. 6080–6097, Jun. 2015, doi: [10.1002/2015jd023287](https://doi.org/10.1002/2015jd023287).
- [3] S. Kang et al., "Linking atmospheric pollution to cryospheric change in the third pole region: Current progress and future prospects," *Nat. Sci. Rev.*, vol. 6, no. 4, pp. 796–809, Jul. 2019, doi: [10.1093/nsr/nwz031](https://doi.org/10.1093/nsr/nwz031).
- [4] Y. Qian, M. G. Flanner, L. R. Leung, and W. Wang, "Sensitivity studies on the impacts of Tibetan plateau snowpack pollution on the Asian hydrological cycle and monsoon climate," *Atmos. Chem. Phys.*, vol. 11, no. 5, pp. 1929–1948, 2011, doi: [10.5194/acp-11-1929-2011](https://doi.org/10.5194/acp-11-1929-2011).
- [5] S. M. Skiles and T. H. Painter, "Assessment of radiative forcing by light-absorbing particles in snow from in situ observations with radiative transfer modeling," *J. Hydrometeorol.*, vol. 19, no. 8, pp. 1397–1409, Aug. 2018, doi: [10.1175/jhm-d-18-0072.1](https://doi.org/10.1175/jhm-d-18-0072.1).
- [6] K. M. Sterle, J. R. McConnell, J. Dozier, R. Edwards, and M. G. Flanner, "Retention and radiative forcing of black carbon in eastern Sierra Nevada snow," *Cryosphere*, vol. 7, no. 1, pp. 365–374, 2013, doi: [10.5194/tc-7-365-2013](https://doi.org/10.5194/tc-7-365-2013).
- [7] C. Sarangi et al., "Dust dominates high-altitude snow darkening and melt over high-mountain Asia," *Nature Climate Change*, vol. 10, no. 11, pp. 1045–1051, 2020.
- [8] S. M. Skiles, M. Flanner, J. M. Cook, M. Dumont, and T. H. Painter, "Radiative forcing by light-absorbing particles in snow," *Nature Climate Change*, vol. 8, no. 11, pp. 965–971, Nov. 2018, doi: [10.1038/s41558-018-0296-5](https://doi.org/10.1038/s41558-018-0296-5).
- [9] J. Svensson et al., "Light-absorption of dust and elemental carbon in snow in the Indian Himalayas and the Finnish Arctic," *Atmos. Meas. Techn.*, vol. 11, no. 3, pp. 1403–1416, Mar. 2018, doi: [10.5194/amt-11-1403-2018](https://doi.org/10.5194/amt-11-1403-2018).
- [10] S. Kaspari, T. H. Painter, M. Gysel, S. M. Skiles, and M. Schwikowski, "Seasonal and elevational variations of black carbon and dust in snow and ice in the Solu-Khumbu, Nepal and estimated radiative forcings," *Atmos. Chem. Phys.*, vol. 14, no. 15, pp. 8089–8103, 2014, doi: [10.5194/acp-14-8089-2014](https://doi.org/10.5194/acp-14-8089-2014).
- [11] P. Bonasoni et al., "Atmospheric brown clouds in the Himalayas: First two years of continuous observations at the Nepal climate observatory-pyramid (5079 m)," *Atmos. Chem. Phys.*, vol. 10, no. 15, pp. 7515–7531, 2010, doi: [10.5194/acp-10-7515-2010](https://doi.org/10.5194/acp-10-7515-2010).
- [12] X. Y. Zhong et al., "Light-absorbing impurities in snow cover across Northern Xinjiang, China," *J. Glaciol.*, vol. 65, no. 254, pp. 940–956, Dec. 2019, doi: [10.1017/jog.2019.69](https://doi.org/10.1017/jog.2019.69).
- [13] F. Zhang et al., "Black carbon and mineral dust in snow cover across a typical city of Northeast China," *Sci. Total Environ.*, vol. 807, Feb. 2022, Art. no. 150397, doi: [10.1016/j.scitotenv.2021.150397](https://doi.org/10.1016/j.scitotenv.2021.150397).
- [14] Y. L. Zhang et al., "Black carbon and mineral dust in snow cover on the Tibetan Plateau," *Cryosphere*, vol. 12, no. 2, pp. 413–431, Feb. 2018, doi: [10.5194/tc-12-413-2018](https://doi.org/10.5194/tc-12-413-2018).
- [15] W. Pu et al., "Properties of black carbon and other insoluble light-absorbing particles in seasonal snow of northwestern China," *Cryosphere*, vol. 11, no. 3, pp. 1213–1233, May 2017, doi: [10.5194/tc-11-1213-2017](https://doi.org/10.5194/tc-11-1213-2017).
- [16] X. Wang, B. Q. Xu, and J. Ming, "An overview of the studies on black carbon and mineral dust deposition in snow and ice cores in East Asia," *J. Meteorol. Res.*, vol. 28, no. 3, pp. 354–370, Jun. 2014, doi: [10.1007/s13351-014-4005-7](https://doi.org/10.1007/s13351-014-4005-7).
- [17] X. Wang et al., "Quantifying the light absorption and source attribution of insoluble light-absorbing particles on Tibetan Plateau glaciers between 2013 and 2015," *Cryosphere*, vol. 13, no. 1, pp. 309–324, Jan. 2019, doi: [10.5194/tc-13-309-2019](https://doi.org/10.5194/tc-13-309-2019).
- [18] Z. Du, C. Xiao, M. Ding, and C. Li, "Identification of multiple natural and anthropogenic sources of dust in snow from Zhongshan Station to Dome A, East Antarctica," *J. Glaciol.*, vol. 64, pp. 855–865, Sep. 2018, doi: [10.1017/jog.2018.72](https://doi.org/10.1017/jog.2018.72).
- [19] J. Kavan, D. Nývlt, K. Láska, Z. Engel, and M. Kňážková, "High-latitude dust deposition in snow on the glaciers of James Ross Island, Antarctica," *Earth Surf. Processes Landforms*, vol. 45, pp. 1569–1578, 2020, doi: [10.1002/esp.4831](https://doi.org/10.1002/esp.4831).
- [20] R. Reynolds et al., "Dust deposited on snow cover in the San Juan Mountains, Colorado, 2011–2016: Compositional variability bearing on snow-melt effects," *J. Geophysical Res., Atmos.*, vol. 125, 2020, Art. no. e2019JD032210, doi: [10.1029/2019JD032210](https://doi.org/10.1029/2019JD032210).
- [21] C. Telloli, M. Chicca, S. Pepi, and C. Vaccaro, "Saharan dust particles in snow samples of Alps and Apennines during an exceptional event of transboundary air pollution," *Environ. Monit. Assessment*, vol. 190, 2017, Art. no. 37, doi: [10.1007/s10661-017-6412-6](https://doi.org/10.1007/s10661-017-6412-6).
- [22] S. C. Kang et al., "Black carbon and organic carbon dataset over the third pole," *Earth Syst. Sci. Data*, vol. 14, no. 2, pp. 683–707, Feb. 2022, doi: [10.5194/essd-14-683-2022](https://doi.org/10.5194/essd-14-683-2022).
- [23] G. A. Grell et al., "Fully coupled 'online' chemistry within the WRF model," *Atmos. Environ.*, vol. 39, no. 37, pp. 6957–6975, 2005.
- [24] S. Chen, J. Huang, C. Zhao, Y. Qian, L. R. Leung, and B. Yang, "Modeling the transport and radiative forcing of Taklimakan dust over the Tibetan Plateau: A case study in the summer of 2006," *J. Geophysical Res., Atmos.*, vol. 118, no. 2, pp. 797–812, 2013.
- [25] L. Liu, X. Huang, A. Ding, and C. Fu, "Dust-induced radiative feedbacks in North China: A dust storm episode modeling study using WRF-Chem," *Atmos. Environ.*, vol. 129, pp. 43–54, 2016.
- [26] J. Zhao, X. Ma, S. Wu, and T. Sha, "Dust emission and transport in Northwest China: WRF-Chem simulation and comparisons with multi-sensor observations," *Atmos. Res.*, vol. 241, 2020, Art. no. 104978.
- [27] T. Aoki, Tadao Aoki, M. Fukabori, A. Hachikubo, Y. Tachibana, and F. Nishio, "Effects of snow physical parameters on spectral albedo and bidirectional reflectance of snow surface," *J. Geophysical Res., Atmos.*, vol. 105, no. D8, pp. 10219–10236, Apr. 2000, doi: [10.1029/1999jd901122](https://doi.org/10.1029/1999jd901122).
- [28] E. Zege, I. Katsev, A. Malinka, A. Prikhach, and I. Polonsky, "New algorithm to retrieve the effective snow grain size and pollution amount from satellite data," *Ann. Glaciol.*, vol. 49, pp. 139–144, 2008, doi: [10.3189/172756408787815004](https://doi.org/10.3189/172756408787815004).
- [29] E. P. Zege, I. L. Katsev, A. V. Malinka, A. S. Prikhach, G. Heygster, and H. Wiebe, "Algorithm for retrieval of the effective snow grain size and pollution amount from satellite measurements," *Remote Sens. Environ.*, vol. 115, no. 10, pp. 2674–2685, Oct. 2011, doi: [10.1016/j.rse.2011.06.001](https://doi.org/10.1016/j.rse.2011.06.001).
- [30] H. Wiebe, G. Heygster, E. Zege, T. Aoki, and M. Hori, "Snow grain size retrieval SGSP from optical satellite data: Validation with ground measurements and detection of snow fall events," *Remote Sens. Environ.*, vol. 128, pp. 11–20, Jan. 2013, doi: [10.1016/j.rse.2012.09.007](https://doi.org/10.1016/j.rse.2012.09.007).
- [31] A. Kokhanovsky, B. Di Mauro, R. Garzonio, and R. Colombo, "Retrieval of dust properties from spectral snow reflectance measurements," *Front. Environ. Sci.*, vol. 9, 2021, Art. no. 644551.
- [32] A. Kokhanovsky, B. Di Mauro, and R. Colombo, "Snow surface properties derived from PRISMA satellite data over the Nansen ice shelf (East Antarctica)," *Front. Environ. Sci.*, vol. 10, pp. 1–13, Sep. 2022, doi: [10.3389/fenvs.2022.904585](https://doi.org/10.3389/fenvs.2022.904585).

- [33] D. H. Shao, W. B. Xu, H. Y. Li, J. Wang, and X. H. Hao, "Reconstruction of remotely sensed snow albedo for quality improvements based on a combination of forward and retrieval models," *IEEE Trans. Geosci. Remote Sens.*, vol. 56, no. 12, pp. 6969–6985, Dec. 2018, doi: [10.1109/Tgrs.2018.2846681](https://doi.org/10.1109/Tgrs.2018.2846681).
- [34] D. H. Shao, W. B. Xu, H. Y. Li, J. Wang, and X. H. Hao, "Modeling snow surface spectral reflectance in a land surface model targeting satellite remote sensing observations," *Remote Sens.*, vol. 12, no. 18, Sep. 2020, Art. no. 3101, doi: [10.3390/rs12183101](https://doi.org/10.3390/rs12183101).
- [35] S. G. Warren and R. E. Brandt, "Optical constants of ice from the ultraviolet to the microwave: A revised compilation," *J. Geophysical Res., Atmos.*, vol. 113, no. D14, 2008, Art. no. D14220.
- [36] G. Picard, Q. Libois, and L. Arnaud, "Refinement of the ice absorption spectrum in the visible using radiance profile measurements in Antarctic snow," *Cryosphere*, vol. 10, no. 6, pp. 2655–2672, 2016.
- [37] J. Wang et al., "Investigation on snow characteristics and their distribution in China," *Adv. Earth Sci.*, vol. 33, no. 1, pp. 12–26, 2018.
- [38] A. A. Kokhanovsky and E. P. Zege, "Scattering optics of snow," *Appl. Opt.*, vol. 43, no. 7, pp. 1589–1602, 2004.
- [39] A. Kokhanovsky et al., "On the reflectance spectroscopy of snow," *Cryosphere*, vol. 12, no. 7, pp. 2371–2382, 2018.
- [40] Z. Hu et al., "Trans-Pacific transport and evolution of aerosols: Evaluation of quasi-global WRF-Chem simulation with multiple observations," *Geosci. Model Develop.*, vol. 9, no. 5, pp. 1725–1746, 2016, doi: [10.5194/gmd-9-1725-2016](https://doi.org/10.5194/gmd-9-1725-2016).
- [41] K. Usha, V. S. Nair, and S. S. Babu, "Modeling of aerosol induced snow albedo feedbacks over the Himalayas and its implications on regional climate," *Climate Dyn.*, vol. 54, pp. 4191–4210, 2020.
- [42] S. Rahimi, X. Liu, C. Zhao, Z. Lu, and Z. J. Lebo, "Examining the atmospheric radiative and snow-darkening effects of black carbon and dust across the Rocky Mountains of the United States using WRF-Chem," *Atmos. Chem. Phys.*, vol. 20, no. 18, pp. 10911–10935, 2020.
- [43] C. Sarangi et al., "Impact of light-absorbing particles on snow albedo darkening and associated radiative forcing over high-mountain Asia: High-resolution WRF-Chem modeling and new satellite observations," *Atmos. Chem. Phys.*, vol. 19, no. 10, pp. 7105–7128, 2019.
- [44] A. Kokhanovsky, "Dust," in *Snow optics*, 3rd ed. Switzerland: Springer, 2021, ch. 4, sec. 4.4.3, pp. 128–131.



Donghang Shao received the B.S. degree in geographical information system from the Hefei University of Technology, Hefei, China, in 2014, the M.S. degree in cartography and geographical information system from the Northwest Institute of Eco-Environment and Resources, Chinese Academy of Sciences, Lanzhou, China, in 2017, and the Ph.D. degree in information and communication engineering from the University of Electronic Science and Technology of China, Chengdu, China, in 2021.

He is currently a Research Assistant with the Northwest Institute of Eco-Environment and Resources, Chinese Academy of Sciences, Lanzhou, China. His research interests include the remote sensing of snow, snow radiative transfer, and snow and climate change.



Hongyi Li received the B.S. degree in geomatics engineering from the China University of Mining Technology, Xuzhou, China, in 2003, and the Ph.D. degree in cartography and geographical information system from Cold and Arid Regions Environmental and Engineering Research Institute, Chinese Academy of Sciences, Lanzhou, China, in 2009.

He is currently a Professor with the Northwest Institute of Eco-Environment and Resources, Chinese Academy of Sciences, Lanzhou, China. His research interests include snow hydrology and remote sensing retrieval of snow parameters. Recent works are snowmelt simulation under complex terrain conditions.



Alexander Kokhanovsky received the B. S. degree in theoretical physics from Physical Department, Belarusian State University, Minsk, Belarus, in 1983, and the Ph.D. degree in optical sciences from the B.I. Stepanov Institute of Physics, National Academy of Sciences of Belarus, Minsk, Belarus, in 1991.

He has worked with several leading research centers, including the Institute of Physics (Minsk, Belarus), NASDA (Tokyo, Japan), Clausthal University (Clausthal-Zellerfeld, Germany), Imperial College (London, U.K.), University of Bremen (Bremen, Germany), EUMETSAT, and TELSPAZIO Belgium (Darmstadt, Germany). He is currently employed by GFZ Potsdam, where he is working with EnMAP data to retrieve snow and ice properties using hyperspectral observations. His research interests are directed toward modeling light propagation and scattering in terrestrial atmosphere and surface, including ice and snow. He published more than 350 papers and seven books in the field of environmental optics, radiative transfer, remote sensing, and light scattering.



Wenzheng Ji received the B.S. degree in remote sensing science and technology from the Chengdu University of Technology, Chengdu, China, in 2020, and the M.S. degree in cartography and geographic information system from the Northwest Institute of Eco-Environment and Resources, Chinese Academy of Sciences, Lanzhou, China, in 2023. He is currently working toward the Ph.D. degree in cartography and geographical information system with the Northwest Institute of Eco-Environment and Resources, Chinese Academy of Sciences.

His research interests include the remote sensing of snow, snow radiative transfer, and snow and climate change.



Xinyue Zhong received the B.S. degree in tourism management from Shenyang Normal University, Shenyang, China, in 2006, the M.S. degree in tourism management from Northwest Normal University, Lanzhou, China, in 2010, and the Ph.D. degree in physical geography from the Northwest Institute of Eco-Environment and Resources, Chinese Academy of Sciences, Lanzhou, in 2014.

She is currently an Associate Professor with the Northwest Institute of Eco-Environment and Resources, Chinese Academy of Sciences, Lanzhou, China. Her research interests include climatology of snow cover, snow observation experiments, and snow ice chemistry.



Haojie Li received the B.S. degree in geographical information system from the Chengdu University of Technology, Chengdu, China, in 2010, and the Ph.D. degree in cartography and geographical information system from the Northwest Institute of Eco-Environment and Resources, Chinese Academy of Sciences, Lanzhou, China, in 2021.

He is currently an Associate Professor with Northwest Normal University, Lanzhou, China. His research interests include hydrology remote sensing in cold region and cryosphere remote sensing. Recent works are remote sensing of river ice in high and cold mountain regions.



Hongxing Li received the B.S. degree in environmental science from Northwest Normal University, Lanzhou, China, in 2004, and the Ph.D. degree in cartography and geographical information system from the Northwest Institute of Eco-Environment and Resources, Chinese Academy of Sciences, Lanzhou, in 2015.

She is currently a Senior Engineer with the Northwest Institute of Eco-Environment and Resources, Chinese Academy of Sciences, Lanzhou, China. Her research interests include the optical remote sensing of snow.



Xiaohua Hao received the B.S. degree in geographical information system from Lanzhou University, Lanzhou, China, in 2003, and the Ph.D. degree in cartography and geographical information system from Cold and Arid Regions Environmental and Engineering Research Institute, Chinese Academy of Sciences, Lanzhou, in 2009.

He is currently a Professor with the Northwest Institute of Eco-Environment and Resources, Chinese Academy of Sciences, Lanzhou, China. His research interests include optical remote sensing of snow, snow radiative transfer, and snow and climate change.